Linking Carbon and Boron–Nitride Nanotubes: Heterojunction Energetics and Band Gap Tuning

ARTICLE *in* JOURNAL OF PHYSICAL CHEMISTRY LETTERS · AUGUST 2010

Impact Factor: 7.46 · DOI: 10.1021/jz100753x

THE JOURNAL OF PHYSICAL CHEMISTRY Letters

pubs.acs.org/JPCL

Linking Carbon and Boron-Nitride Nanotubes: Heterojunction Energetics and Band Gap Tuning

Wei An and C. Heath Turner*

Department of Chemical and Biological Engineering, The University of Alabama, Box 870203, Tuscaloosa, Alabama 35487-0203

ABSTRACT We investigate the energetics of forming heteronanotubes, which are combinations of pure carbon nanotube (CNT) segments and boron-nitride nanotube (BNNT) segments. Our density functional theory calculations predict that the adverse impacts of heterojunctions on the nanotube stability can be minimized if the CNT and/or the BNNT building block segments are sufficiently large along the axial direction (corresponding to circular junctions). As such, carbon−boron-nitride heteronanotubes can be thermodynamically competitive in stability, as compared to pure CNTs and BNNTs of similar geometry, and this is in good agreement with previous experimental observations. In addition, we find that the highest occupied crystal orbital/lowest unoccupied crystal orbital (HOCO−LUCO) gap of carbon−boron-nitride heteronanotubes can be significantly tuned by modifying the CNT and BNNT combinations, the tube chirality, or the junction geometry (i.e., circular or linear).

SECTION Nanoparticles and Nanostructures

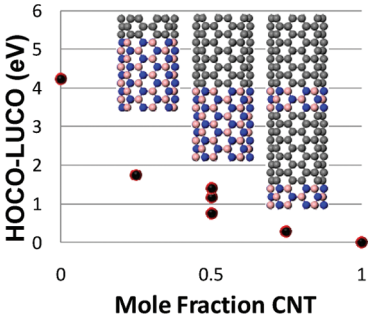

Carbon nanotubes (CNTs) are known to be intrinsically either semiconducting or metallic, depending upon the chirality of the nanotube.[1] Boron-nitride nanotubes (BNNTs) are electrical insulators, with a large band gap of ca. 5.5 eV (independent of their chirality).[2] Due to the exciting, yet distinct properties discovered in CNTs and BNNTs,[3−5] a number of research groups have begun to explore combinations of these component materials in order to develop hybrid structures (i.e., CBNNTs) with desirable properties.[6−17] In particular, the combination of these building blocks may allow the fundamental control needed for designing next-generation electronic components, sensors, and structural composites.

The hybrid nanotubes can be ideally constructed from two basic geometries: (1) alternating segments of CNT and BNNT (with radial junctions); or (2) continuous segments of CNT and BNNT, with each segment corresponding to one-half of the radial composition (resulting in two linear junctions along the tube axis). However, the most common forms of CBNNTs that are observed in experiments can be characterized as BN-doped CNTs, with little control over the BN pattern formation. In general, there is a tendency toward compositional segregation into homogeneous regions of carbon and separate regions of boron-nitride.

Previous density functional theory (DFT) studies[11−17] have shown that the electronic structure of hybrid CBNNTs depends on the pattern and the composition of C and BN within the tube lattice. Relatively large, ternary heteronanotubes with sequential C and BN segments have been experimentally realized via self-organization, using laser vaporization methods (assisted by Co/Ni catalyst under N_2 atmosphere).[9,10] However, the effect of the heterojunctions (in terms of the number and composition) on the growth, stability, and the electronic structure of the resulting heteronanotubes, is still unknown. This information is necessary when designing optimal synthesis procedures for these structures and for understanding their resulting properties, which may be tuned for specific applications.

In order to provide more fundamental information about these hybrid materials, we have performed DFT calculations on ternary carbon−boron-nitride heteronanotubes using the VASP electronic structure code (see Supporting Information for computational methods). In our calculations, prototype C and BN single-walled nanotubes (CBNNTs), corresponding to zigzag (8,0) and armchair (6,6) structures, were chosen to model the general features of these hybrid materials, as shown in Figures 1 and 2.

Here, we define two distinct structural combinations of CNTs with BNNTs to be used in our modeling investigation: (1) alternating segments of CNT and BNNT (with radial junctions perpendicular to the tube axis); and (2) continuous segments of CNT and BNNT, with each segment corresponding to one-half of the radial composition (resulting in two linear junctions, parallel to the tube axis). While many other arrangements can be imagined, we focus on these two well-defined geometric linkages, in order to establish well-characterized benchmarks for future work. The connection between the carbon segments and boron-nitride segments is referred to here as a "heterojunction", and these connections are an important focus of our modeling work. We abbreviate the first

Received Date: June 3, 2010
Accepted Date: July 1, 2010

DOI: 10.1021/jz100753x | J. Phys. Chem. Lett. 2010, 1, 2269–2273

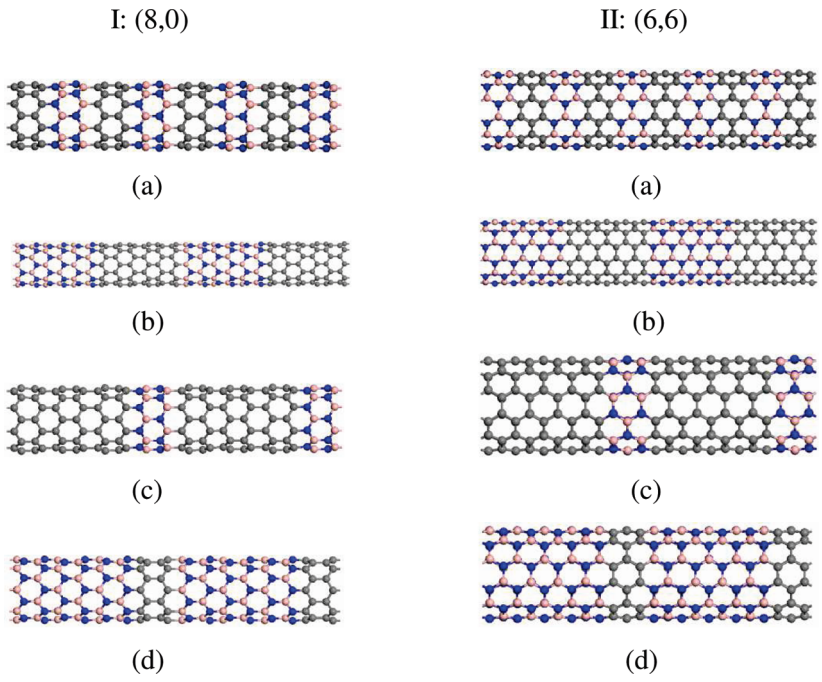

Figure 1. Column I: side view of ternary (8,0) $C_x|(BN)_y$ heteronanotubes: (a) $C_1|(BN)_1$; (b) $C_3|(BN)_3$; (c) $C_3|(BN)_1$; (d) $C_1|(BN)_3$. Column II: side view of ternary (6,6) $C_x|(BN)_y$ heteronanotubes: (a) $C_{1.5}|(BN)_{1.5}$; (b) $C_{4.5}|(BN)_{4.5}$; (c) $C_{4.5}|(BN)_{1.5}$; (d) $C_{1.5}|(BN)_{4.5}$. As a guide to the eye, multiple unit cells are shown. KEY: carbon (gray), nitrogen (blue), and boron (pink).

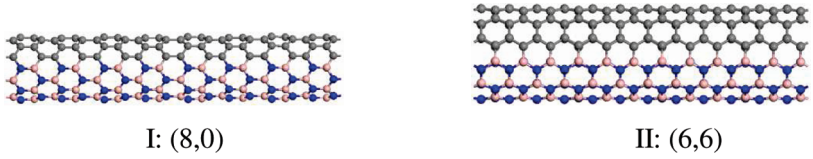

Figure 2. Side view of ternary C−BN (8,0) and (6,6) heteronanotubes, represented in columns I and II, respectively. As a guide to the eye, multiple unit cells are shown. KEY: carbon (gray), nitrogen (blue), and boron (pink).

hybrid structure (with alternating segments) as $C_x|(BN)_y$, with x and y indicating the lengths of the constituent segments (see Figure 1). The second structure (with continuous segments) is abbreviated as C−BN (see Figure 2).

It is known that single-walled (8,0) and (6,6) CNTs (SWCNTs) are semiconducting and metallic, respectively, while single-walled (8,0) and (6,6) BNNTs (SWBNNTs) are both semiconducting. Thus, combinations of these materials should lead to materials with tunable electronic structures, depending upon the specific geometry and fractions of the material components. In order to quantify the electronic properties of each CBNNT, we calculate the density of states (DOS) of each structure, as well as the highest occupied crystal orbital/lowest unoccupied crystal orbital (HOCO−LUCO) gap.

As shown in Figure 1, both zigzag and armchair $C_x|(BN)_y$ heteronanotubes can be generated as nearly seamless tubular structures via hybrid connections (i.e., C−N and C−B covalent bonds), regardless of the various x and y values. However, due to lattice mismatch and strain at the heterojunctions, the formation of $C_x|(BN)_y$ heteronanotubes is energetically less favorable, as compared to that of pristine CNTs and BNNTs with the same basic geometry (see Figure 3). The formation energies are defined as the total energy of the nanotube minus the energy summation of the individual atoms in the gas phase, reported in electron volts per atom. The formation energy decreases (i.e., becomes more exothermic) with respect to x and y. The formation energies (or binding energies) predict the relative stability of hybrid CBNNT heteronanotubes, as those with more negative values should be more stable. These values are expected to ultimately converge to those of a mixture of pristine CNTs and BNNTs, −7.31 and −7.38 eV/atom, respectively (as shown by the dashed line in Figure 3). The calculated formation energies for C−(BN) (8,0) and (6,6) heteronanotubes are −7.26 and −7.31 eV/atom, respectively, and these values are expected to persist in longer nanotubes, since these heterojunctions run parallel to the tube axis. Entropic contributions were not considered in our energy comparisons, as the entropy contributions are expected to be similar among these hybrid structures.

It can be seen that the formation of $C_x|(BN)_y$ heterojunctions has an adverse impact on the stability of the heteronanotubes. As the values of x and y decrease, there is an increase in the number of junctions per unit length, and this results in an increasing energetic penalty. Due to their larger diameter (8.22 vs 6.38 Å),[18] (6,6) heteronanotubes exhibit a smaller energy penalty, as compared to the formation of (8,0)

DOI: 10.1021/jz100753x | J. Phys. Chem. Lett. 2010, 1, 2269–2273

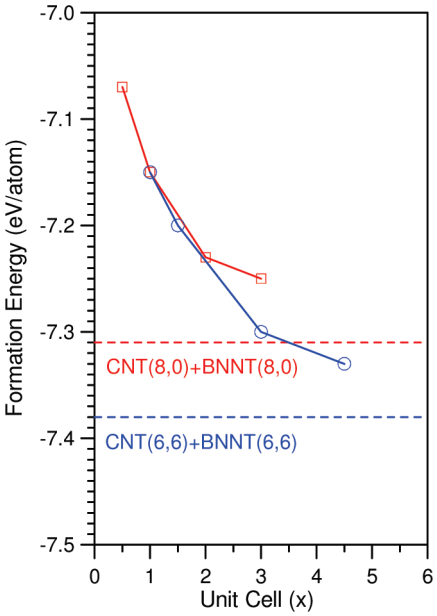

Figure 3. Formation energy of ternary $C_x|(BN)_y$ heteronanotubes as a function of the number of unit cells (x) comprising each section, with $x = y$. As a reference, the composition per unit cell of (8,0) and (6,6) heteronanotubes is $[C_{32}B_{16}N_{16}]$ and $[C_{24}B_{12}N_{12}]$, respectively.

heteronanotubes. On the basis of our calculations, it is estimated that the energy penalty of heterojunctions in (8,0) and (6,6) $C_x|(BN)_y$ nanotubes converges to 0.24 and 0.23 eV/atom per junction, respectively. As compared to the sizes of the $C_x|(BN)_y$ structures synthesized in experiments, the x and y values employed in our models are much smaller. Thus, the converged values that we report should represent the maximum energy penalty with respect to the experimentally relevant energy values. From Figure 3, one can easily project that the $C_x|(BN)_y$ heteronanotubes with increasing segment lengths (i.e., fewer junctions per length) will be thermodynamically competitive with the corresponding CNTs and BNNTs. This provides a supporting explanation for the experimental observations of $C_x|(BN)_y$ formation via catalyst-assisted growth. The compositional segregation observed in experiments can be attributed to the energy penalty of the heterojunctions.

In Figure 4, we show the calculated total DOS for (8,0) and (6,6) CBNNT heteronanotubes, with both $C_x|(BN)_y$ and C−BN linkages. As shown in Figure 4f,g, our calculated DOS values agree with the consensus that SWCNT (8,0) and (6,6) are semiconducting and metallic, respectively, whereas SWBNNT (8,0) and (6,6) are both semiconducting. From Figure 4(I), which corresponds to (8,0) nanotubes, one can see that $C_1|(BN)_1$ and $C_1|(BN)_3$ become more semiconducting with

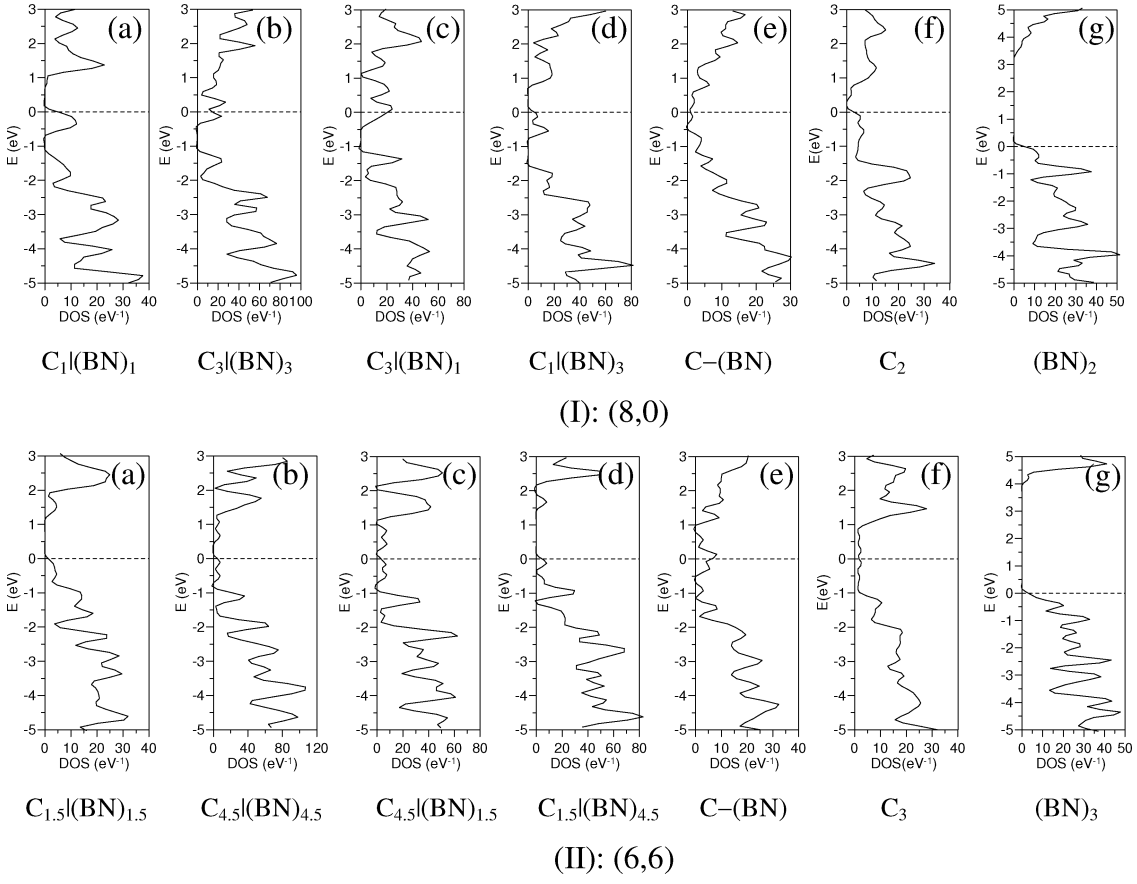

Figure 4. Calculated total DOS for the ternary carbon−boron-nitride heteronanotubes shown in Figure 1. Row I: (8,0); Row II: (6,6). Parts f and g are DOSs for pristine CNT and BNNT. The Fermi level (dashed line) is shifted to 0 eV.

DOI: 10.1021/jz100753x | J. Phys. Chem. Lett. 2010, 1, 2269–2273

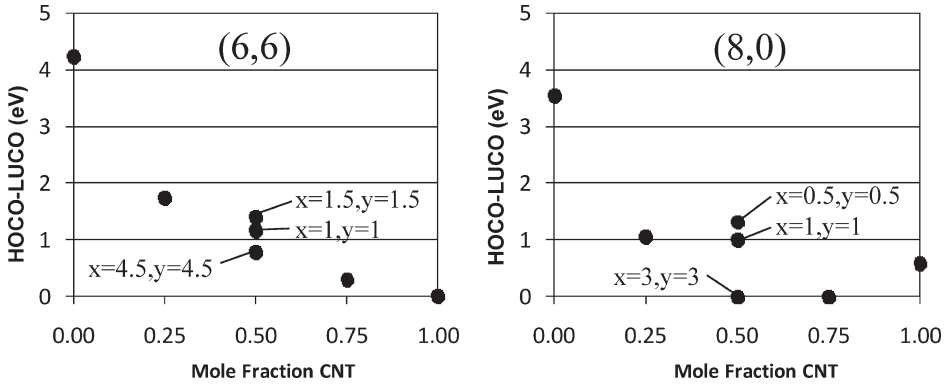

Figure 5. The HOCO−LUCO gaps (eV) of CBNNTs as a function of the mole fraction of the CNT segment, with (6,6) nanotubes on left and (8,0) nanotubes on right. Multiple data points are shown at CNT mole fractions of 0.50. These points correspond to models with different lengths of the CNT and BNNT sections, corresponding to $C_x|(BN)_y$, as shown.

increased HOCO−LUCO (HL) gaps (i.e., 1.00 and 1.06 eV, respectively), as compared to pristine SWCNT (8,0) (i.e., 0.59 eV). However, $C_3|(BN)_3$ and $C_3|(BN)_1$ become metallic with significant electron states populated at the Fermi level, and C−(BN) also becomes slightly metallic. As a reference, zigzag BNNT (8,0) has a calculated HL gap of 3.55 eV in this work.

From Figure 4(II)a−d, which corresponds to (6,6) nanotubes, all of the heteronanotubes demonstrate semiconducting behavior, with HL gaps of 1.42, 0.78, 0.30, and 1.75 eV, respectively. It is apparent that the semiconducting nature of armchair BNNT (6,6), with an HL gap of 4.25 eV, plays a significant role in the resulting electronic properties of the $C_x|(BN)_y$ (6,6) heteronanotubes. In contrast, the C−(BN) (6,6) heteronanotube remains metallic, with enhanced conductivity. This is evident from the additional states formed at the Fermi level, as compared to the pristine SWCNT (6,6), and this can be seen by comparing parts e and f of Figure 4(II).

Overall, we find that the electronic structure of ternary CBNNTs can be tuned by modifying the composition and size of the C_x and/or the $(BN)_y$ units, leading to either more metallic or more semiconducting behavior. This can be clearly seen in Figure 5, which shows the HOCO−LUCO gap as a function of the CBNNT composition. From the projected DOS (not shown), we also find that the states around the Fermi level are *not* mainly associated with the interfacial C, B, and N states at the heterojunctions, but rather, these states are contributed from the whole lattice structure. In addition, our initial studies indicate that the tuneability of zigzag and armchair $C_x|(BN)_y$ electronic properties appears to be different, as shown in Figure 5. It is worth mentioning that the PBE functional employed in our calculations is known to underestimate the band gap of semiconducting CNTs. However, the metallic or semiconducting nature and the trend in the HOCO−LUCO gaps identified by our DFT calculations should be consistent.[19] Additionally, the energy values and electronic structures obtained from the PBE functional should be sufficient to identify the trends in the relative stability and electronic properties of the CBNNT heteronanotubes.

In summary, we have investigated the stability and electronic structure of carbon−boron-nitride heteronanotubes using DFT calculations. We predict that $C_x|(BN)_y$ heteronanotubes with fewer nodes (per unit length) can be thermodynamically competitive in stability with the corresponding pristine CNTs and BNNTs. Moreover, the HOCO−LUCO gap of the heteronanotubes can be tuned by modifying the x and y combinations, the tube chirality, and the junction geometry (either parallel or perpendicular to the tube axis). These results may guide future experimental synthesis of functional materials or help rationalize future experimental results of BCN heteronanotubes.

SUPPORTING INFORMATION AVAILABLE Computational methods. This material is available free of charge via the Internet at http://pubs.acs.org.

AUTHOR INFORMATION

Corresponding Author:

*To whom correspondence should be addressed. E-mail: hturner@eng.ua.edu; phone: 205-348-1733; fax: 205-348-7558.

ACKNOWLEDGMENT Funding for this work has been provided by an NSF CAREER Award (#0747690). Supercomputer resources were provided by the Alabama Supercomputer Center, NCSA TeraGrid. A portion of the research was performed using EMSL, a national scientific user facility sponsored by the Department of Energy's Office of Biological and Environmental Research and located at Pacific Northwest National Laboratory.

REFERENCES

(1) Wildoer, J. W. G.; Venema, L. C.; Rinzler, A. G.; Smalley, R. E.; Dekker, C. Electronic Structure of Atomically Resolved Carbon Nanotubes. *Nature* **1998,** *391*, 59–62.

(2) Blase, X.; Rubio, A.; Louie, S. G.; Cohen, M. L. Stability and Band-Gap Constancy of Boron-Nitride Nanotubes. *Europhys. Lett.* **1994,** *28*, 335–340.

(3) Baughman, R. H.; Zakhidov, A. A.; de Heer, W. A. Carbon Nanotubes - The Route Toward Applications. *Science* **2002,** *297*, 787–792.

(4) Terrones, M.; Romo-Herrera, J. M.; Cruz-Silva, E.; Lopez-Urias, F.; Munoz-Sandoval, E.; Velazquez-Salazar, J. J.; Terrones, H.; Bando, Y.; Golberg, D. Pure and Doped Boron Nitride Nanotubes. *Mater. Today* **2007,** *10*, 30–38.

(5) Golberg, D.; Bando, Y.; Tang, C. C.; Zhi, C. Y. Boron Nitride Nanotubes. *Adv. Mater.* **2007,** *19*, 2413–2432.

DOI: 10.1021/jz100753x | *J. Phys. Chem. Lett.* **2010,** *1*, 2269–2273

(6) Zhi, C. Y.; Bando, Y.; Tang, C. C.; Kuwahara, H.; Golberg, D. Grafting Boron Nitride Nanotubes: From Polymers to Amorphous and Graphitic Carbon. *J. Phys. Chem. C* **2007,** *111*, 1230–1233.
(7) Wang, W. L.; Bai, X. D.; Liu, K. H.; Xu, Z.; Golberg, D.; Bando, Y.; Wang, E. G. Direct Synthesis of B−C−N Single-Walled Nanotubes by Bias-Assisted Hot Filament Chemical Vapor Deposition. *J. Am. Chem. Soc.* **2006,** *128*, 6530–6531.
(8) Wang, W. L.; Bando, Y.; Zhi, C. Y.; Fu, W. Y.; Wang, E. G.; Golberg, D. Aqueous Noncovalent Functionalization and Controlled Near-Surface Carbon Doping of Multiwalled Boron Nitride Nanotubes. *J. Am. Chem. Soc.* **2008,** *130*, 8144–8145.
(9) Enouz, S.; Stephan, O.; Cochon, J. L.; Colliex, C.; Loiseau, A. C−BN Patterned Single-Walled Nanotubes Synthesized by Laser Vaporization. *Nano Lett.* **2007,** *7*, 1856–1862.
(10) Enouz-Vedrenne, S.; Stephan, O.; Glerup, M.; Cochon, J. L.; Colliex, C.; Loiseau, A. Effect of the Synthesis Method on the Distribution of C, B, and N Elements in Multiwall Nanotubes: A Spatially Resolved Electron Energy Loss Spectroscopy Study. *J. Phys. Chem. C* **2008,** *112*, 16422–16430.
(11) Zhang, Z. Y.; Zhang, Z. H.; Guo, W. L. Stability and Electronic Properties of a Novel C−BN Heteronanotube from First-Principles Calculations. *J. Phys. Chem. C* **2009,** *113*, 13108–13114.
(12) Du, A. J.; Chen, Y.; Zhu, Z. H.; Lu, G. Q.; Smitht, S. C. C−BN Single-Walled Nanotubes from Hybrid Connection of BN/C Nanoribbons: Prediction by Ab Initio Density Functional Calculations. *J. Am. Chem. Soc.* **2009,** *131*, 1682–1683.
(13) Pan, H.; Feng, Y. P.; Lin, J. Y. Ab Initio Study of Single-Wall BC_2N Nanotubes. *Phys. Rev. B* **2006,** *74*, 045409.
(14) Cho, Y. J.; Kim, C. H.; Kim, H. S.; Park, J.; Choi, H. C.; Shin, H. J.; Gao, G.; Kang, H. S. Electronic Structure of Si-Doped BN Nanotubes Using X-ray Photoelectron Spectroscopy and First-Principles Calculation. *Chem. Mater.* **2009,** *21*, 136–143.
(15) Kim, S. Y.; Park, J.; Choi, H. C.; Ahn, J. P.; Hou, J. Q.; Kang, H. S. X-ray Photoelectron Spectroscopy and First Principles Calculation of BCN Nanotubes. *J. Am. Chem. Soc.* **2007,** *129*, 1705–1716.
(16) Choi, J.; Kim, Y. H.; Chang, K. J.; Tomanek, D. Itinerant Ferromagnetism in Heterostructured C/BN Nanotubes. *Phys. Rev. B* **2003,** *67*, 125421.
(17) Miyamoto, Y.; Rubio, A.; Cohen, M. L.; Louie, S. G. Chiral Tubules of Hexagonal BC_2N. *Phys. Rev. B* **1994,** *50*, 4976–4979.
(18) An, W.; Turner, C. H. Chemisorption of Transition-Metal Atoms on Boron- and Nitrogen-Doped Carbon Nanotubes: Energetics and Geometric and Electronic Structures. *J. Phys. Chem. C* **2009,** *113*, 7069–7078.
(19) Avramov, P. V.; Kudin, K. N.; Scuseria, G. E. Single Wall Carbon Nanotubes Density of States: Comparison of Experiment and Theory. *Chem. Phys. Lett.* **2003,** *370*, 597–601.

DOI: 10.1021/jz100753x | *J. Phys. Chem. Lett.* **2010,** *1*, 2269–2273